

# Fluctuations and Randomness of Movement of the Bead Powered by a Single Kinesin Molecule in a Force-Clamped Motility Assay: Monte Carlo Simulations

Yi-der Chen, Bo Yan, and Robert J. Rubin

Mathematical Research Branch, National Institute of Diabetes, Digestive and Kidney Diseases, National Institutes of Health, Bethesda, Maryland 20892-2690 USA

**ABSTRACT** The motility assay of K. Visscher, M. J. Schnitzer, and S. M. Block (*Nature*, 400:184–189, 1999) in which the movement of a bead powered by a single kinesin motor can be measured is a very useful tool in characterizing the *force-dependent* steps of the mechanochemical cycle of kinesin motors, because in this assay the external force applied to the bead can be controlled (clamped) arbitrarily. However, because the bead is elastically attached to the motor and the response of the clamp is not fast enough to compensate the Brownian motion of the bead, interpretation or analysis of the data obtained from the assay is not trivial. In a recent paper (Y. Chen and B. Yan, *Biophys. Chem.* 91:79–91, 2001), we showed how to evaluate the *mean* velocity of the bead and the motor in the motility assay for a given mechanochemical cycle. In this paper we extend the study to the evaluation of the *fluctuation* or the *randomness* of the velocity using a Monte Carlo simulation method. Similar to the mean, we found that the randomness of the velocity of the motor is also influenced by the parameters that affect the dynamic behavior of the bead, such as the viscosity of the medium, the size of the bead, the stiffness of the elastic element connecting the bead and the motor, etc. The method presented in this paper should be useful in modeling the kinetic mechanism of any processive motor (such as conventional kinesin and myosin V) based on measured force-clamp motility data.

## INTRODUCTION

Two-headed conventional kinesins are microtubule-activated ATPases that can use the free energy of ATP hydrolysis to carry a cargo and move processively along a microtubule (MT). It is generally believed that the mechanical translocation of kinesins on an MT proceeds by a hand-over-hand mechanism (Cross, 1995; Gelles et al., 1995; Peskin and Oster, 1995; Romberg et al., 1998; Hancock and Howard, 1999; Schief and Howard, 2001), in which one head is always attached to the MT while the other head is free to search for the binding site in the forward direction and the binding of the free head facilitates the dissociation of the bound head. That is, in this model the two heads move symmetrically and cooperatively in carrying out the ATP-hydrolysis-induced mechanical translocation of the motor (and the cargo). The hand-over-hand model has also been suggested for actin-based processive motors, such as myosin V (Rief et al., 2000; Mehta, 2001). Recently, the structural element responsible for carrying out this hand-over-hand mechanism in conventional kinesin motors has been suggested (Rice et al., 1999).

The pathway describing the coupling between ATP hydrolysis and translocation of the motor is called the “mechanochemical” cycle of the motor. It has been shown recently (Schnitzer et al., 2000; Fisher and Kolomeisky, 2001) that the mechanochemical cycle of

two-headed kinesin motors can be elucidated using the data obtained from the motility assay of Visscher, Schnitzer, and Block (1999) (referred to as the VSB assay/data from now on), in which the movement of a large bead connected with an elastic spring to a single moving kinesin molecule can be monitored as a function of ATP concentrations in the presence of a force clamp. The method used to deduce the kinetic mechanism of the cycle in these studies is based on the so-called “chemical-kinetic” (CK) formalism in which the effect of the Brownian motion of the bead on the turnover rate of the motor is completely ignored (Qian, 1997, 2000; Kolomeisky and Widom, 1998; Fisher and Kolomeisky, 1999a, b; Schnitzer et al., 2000). In other words, the force exerted on the motor by the bead through the spring is assumed to be constant and equal to the externally applied force. As one can see from Fig. 1 *b* and *c* of Visscher et al. (1999) and will be shown below, the force exerted on the motor is not constant, but fluctuates randomly. This is due to the fact that the force-clamp applied to the bead in the assay is not fast enough to compensate the Brownian motion of the bead. Because the load-dependent rate constants of the cycle are nonlinear functions of the force exerted on the motor, the fluctuation in the force should have an effect on the cycling turnover rate of the motor. In a recent paper (Chen and Yan, 2001; referred to as paper I from now on), we derived a semi-analytic formalism that can be used to calculate the *mean* velocity of the motor (and the bead) for a given mechanochemical cycle without neglecting the Brownian motion of the bead. Using a simple two-state model, we showed that Brownian motion of the bead did have an

---

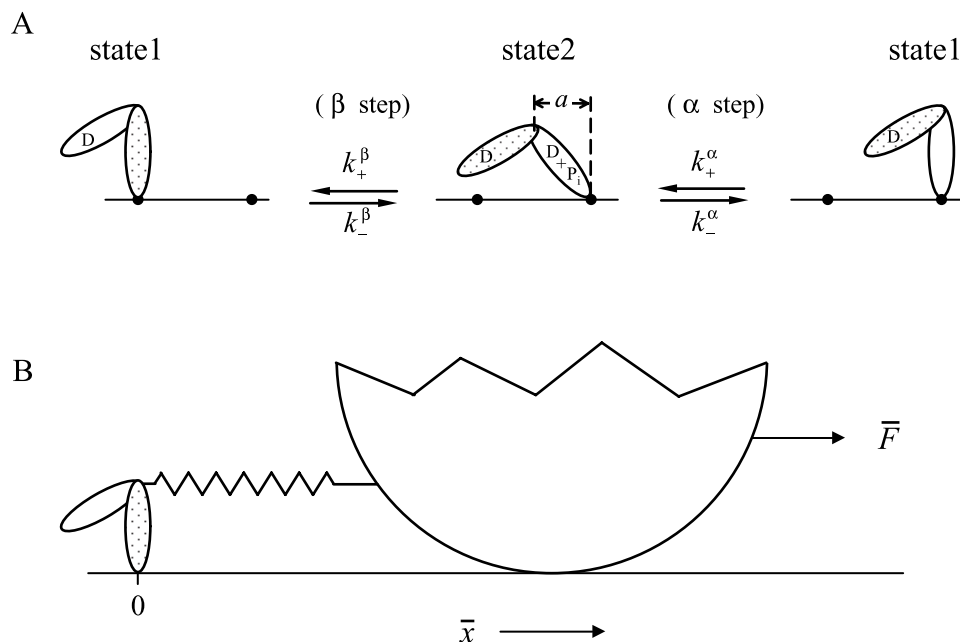
Submitted January 30, 2002/and accepted for publication July 10, 2002.

Address reprint requests to: Yi-der Chen, NIH/NIDDK/MRB, BSA Building, Suite 350, 9000 Rockville Pike, Bethesda, MD 20892-2690. Tel.: 301-496-5436; Fax: 301-402-0535; E-mail: ydchen@helix.nih.gov.

© 2002 by the Biophysical Society

0006-3495/02/11/2360/10 \$2.00

FIGURE 1 (A). Schematic representation of the kinetic mechanisms of the two-state hand-over-hand model. The two-headed motor can exist in two states and undergo two “power” strokes,  $\alpha$  and  $\beta$  steps, when walking from right to left. The neck of the motor moves toward the left by a distance  $\alpha$  (normalized by dividing by the length of the lattice spacing,  $L$ ) when a forward  $1 \rightarrow 2$  transition is executed and by a distance of  $1-\alpha$  when a forward  $2 \rightarrow 1$  transition is executed. Rate constant  $k_+^\alpha$  is proportional to the concentration of ATP and  $k_-^\beta$  is proportional to the concentrations of ADP and  $P_i$ . (B). Schematic representation of the assay of Visscher et al. (1999). The external force,  $F$ , applied to the bead is kept constant.



effect on the rate of translocation of the kinesin on the microtubule and that the estimate of the velocity based on the CK formalism was always an overestimate. However, the formalism is applicable only to the *mean* velocity of the motor; it cannot be used to calculate higher moments of the movement, such as the *fluctuation* or the *randomness* of the velocity. Since randomness was measured by Visscher et al. (1999) and has been shown to be useful for model differentiation (Svoboda and Block, 1994; Schnitzer and Block, 1995), we thought it worthwhile to develop a method to study this quantity. In this paper we present a Monte Carlo procedure to simulate directly the dynamic behaviors of the motor and the bead so that both the *mean* and the *fluctuation* of the velocity of the motor can be evaluated. We show that, similar to what we found for the mean velocity in paper I, the *randomness* of the motor velocity is also affected by the diffusion coefficient of the bead and the stiffness of the spring that govern the Brownian motion of the bead. We also show that randomness evaluated using the present method is different from that based on the CK formalism. Furthermore, fluctuations of the strain and the force (stress) generated in the spring caused by the Brownian motion of the bead are also investigated. By analyzing the statistical properties of the force fluctuation as a function of  $D$  (the diffusion coefficient of the bead) and  $K$  (the stiffness of the elastic spring), we are able to discuss the mechanism by which these two parameters affect the motor movement. We first present the mathematical basis of the method and then discuss the simulation results for a simple two-state hand-over-hand model for kinesin motors.

## MODEL AND METHOD

### The model and its strain-dependent rate constants

As in paper I, we use the simple two-state mechanochemical cycle shown in Fig. 1 A to derive the Monte Carlo simulation procedure. The procedure can be easily extended to more than two states. As described in Fig. 1 A, the two-headed motor is always attached to the microtubule and can exist in states 1 and 2 specified by the bound nucleotide on each head and the “mechanical” conformation of the motor. The word “mechanical” is used here to emphasize that transitions between two *different* mechanical states result in translocations of the cargo or the motor itself. For simplicity, we have chosen the *coordinate* of the “neck” of the motor (where the two heads are joined) to specify the mechanical conformation of the motor. Thus, as shown in Fig. 1 A, in state 1 the coordinate of the neck coincides with that of the site to which the head is attached and the neck is displaced by  $\bar{a}$  in the forward direction from the binding site in state 2. In this model, there are two kinds of transitions between states 1 and 2:  $\alpha$  and  $\beta$  transitions. In the  $\alpha$  transition, the bound head remains attached to the same-binding site on the microtubule, while in the  $\beta$  transition the bound head is detached from the binding site and the free head is attached to the neighboring site at the same time. Thus, a forward  $\alpha$  transition (toward the plus end of the MT for conventional kinesins) results in a linear displacement of the neck by a length of  $\bar{a}$  along the axis of the microtubule in the forward direction. However, a forward  $\beta$  transition results in a forward displacement of  $L - \bar{a}$ , where  $L$  is the length of a tubulin dimer ( $\sim 8$  nm). One must note that, in this simple two-state model, both transitions are *load-dependent*. In a more complicated model with more than two states, some transitions may not depend on the load.

Let  $z$  be the *strain* and  $E(z)$  the energy of the spring at  $z$ . Then, if the spring obeys Hooke’s law (Coppin et al., 1997; Svoboda and Block, 1994; Kojima et al., 1997), we have

$$E(z) = \frac{1}{2}Kz^2 \quad (1)$$

where  $K$  is the elastic coefficient of the spring (see below for a discussion on the actual definition of  $K$ ). As used before in paper I, symbols with a bar above represent the actual physical quantities with dimensions and those

without the bar are dimensionless quantities. Thus, the  $z$ ,  $K$ , and  $E(z)$  here are related to their respective physical quantities as  $z = \bar{z}/L$ ,  $K = \bar{K}L^2/k_B T$ ,  $E(z) = \bar{E}(z)/k_B T$ ; where  $k_B$  is the Boltzmann constant and  $T$  is the absolute temperature. Let  $k_+^\alpha$  ( $\equiv \bar{k}_+^\alpha L^2/D$ , where  $D$  is the diffusion coefficient of the bead) and  $k_-^\alpha$ , respectively, be the dimensionless rate constants of the forward and backward  $\alpha$  transitions *in the absence of the spring (and the bead)* as shown in Fig. 1 A. Then, as in paper I, we assume that the rate constants for the two  $\alpha$  transitions in the presence of the spring between state 1 with strain  $z$  and state 2 with strain  $z + a$  can be expressed as

$$\begin{aligned}\alpha_+(z) &= k_+^\alpha \exp\{\delta_\alpha[E(z) - E(z + a)]\} \\ \alpha_-(z + a) &= k_-^\alpha \exp\{[\delta_\alpha - 1][E(z) - E(z + a)]\}\end{aligned}\quad (2)$$

where  $\delta_\alpha$  is a constant that determines the division of the elastic energy between the forward and the backward rate constants. Note that  $a = \bar{a}/L$  is the dimensionless strain difference between states 1 and 2 for the  $\alpha$  transition. Similar expressions can be written down for the  $\beta$  transitions. With the substitution of Eq. 1, the four rate constants can be expressed as a function of strain  $z$  as

$$\begin{aligned}\alpha_+(z) &= k_+^\alpha e^{-K a \delta_\alpha (2z + a)/2} \\ \alpha_-(z) &= k_-^\alpha e^{K a (1 - \delta_\alpha)(2z - a)/2} \\ \beta_+(z) &= k_+^\beta e^{-K (1 - a) \delta_\beta (2z - a + 1)/2} \\ \beta_-(z) &= k_-^\beta e^{K (1 - a)(1 - \delta_\beta)(2z + a - 1)/2}\end{aligned}\quad (3)$$

Note that we have expressed all four rate constants as a function of  $z$  here (not as a function of  $z$  and  $z + a$ , respectively, as in Eq. 2 to make them ready for simulation. Also note that some of the rate constants in Eqs. 3 are different from those in Eqs. 14 of paper I, because  $z$  refers to the strain of the spring here while  $x$  represents the coordinate of the bead in a special coordinate system described in paper I. Thus, if the transition originates from state 1 (such as the  $\alpha_+$  and  $\beta_-$  reactions), we have  $z = x$  and the rate constants of the two systems are identical. However, if the transition originates from state 2 (the  $\alpha_-$  and  $\beta_+$  reactions), then these two parameters are related by the relation  $z = x + a$ . The rate constants in Eqs. 3 are the basic quantities needed in simulating the cycling kinetics of the motor. Due to the Brownian motion of the bead,  $z$  is not constant but fluctuates randomly as a function of time. As a result, the rate constants in Eqs. 3 are also random variables. In the next section, we show how to evaluate this  $z(t)$ .

## Evaluation of $z(t)$ : the time-dependent strain of the spring between state transitions of the motor

Consider the system in Fig. 1 B where a Brownian bead subject to a constant external force  $\bar{F}$  is connected with an elastic spring to a motor held fixed at  $\bar{x} = 0$ . Let  $\bar{x}(t)$  be the position of the bead at time  $t$ . Then the strain of the spring can be expressed as  $\bar{z}(t) = \bar{x}(t) - \bar{x}_0$  where  $\bar{x}_0$  is the position of the bead at zero strain and the Brownian motion of the bead in this system can be described by the Langevin equation:

$$m \frac{d^2 \bar{x}}{dt^2} + \varsigma \frac{d\bar{x}}{dt} = \bar{F} - \bar{K}(\bar{x} - \bar{x}_0) + \Gamma'(\bar{t})\quad (4)$$

Here  $m$  and  $\varsigma$  ( $\equiv k_B T/D$ ) are respectively the mass and the friction coefficient of the bead and  $\Gamma'(\bar{t})$  is the Langevin force:

$$\langle \Gamma'(\bar{t}) \rangle = 0$$

$$\langle \Gamma'(\bar{t}) \Gamma'(\bar{t}') \rangle = 2\varsigma k_B T \delta(\bar{t} - \bar{t}').$$

If the time of interest is long compared to  $\varsigma/m$  (when the medium is at a low Reynolds number), the acceleration term in Eq. 4 can be neglected and we have

$$\varsigma(d\bar{z}/d\bar{t}) = \bar{F} - \bar{K}\bar{z} + \Gamma'(\bar{t})\quad (5)$$

Let us define a new Langevin force  $\Gamma(\bar{t})$  as

$$\Gamma(\bar{t}) = (2\varsigma k_B T)^{-1/2} \Gamma'(\bar{t}).$$

Then, we have

$$\langle \Gamma(\bar{t}) \rangle = 0,$$

and

$$\langle \Gamma(\bar{t}) \Gamma(\bar{t}') \rangle = (2\varsigma k_B T)^{-1} \langle \Gamma'(\bar{t}) \Gamma'(\bar{t}') \rangle = \delta(\bar{t} - \bar{t}').$$

And the Langevin equation in Eq. 5 becomes

$$d\bar{z}/d\bar{t} = (D/k_B T)[\bar{F} - \bar{K}\bar{z}] + \sqrt{2D}\Gamma(\bar{t})\quad (6)$$

Equation 6 is the stochastic differential equation we want to solve for  $\bar{z}(t)$  when  $\bar{z}(0)$  at time zero is given. Note that if the spring does not obey Hooke's law (Eq. 1), then the  $\bar{K}\bar{z}$  term in Eq. 6 is replaced by  $d\bar{E}/d\bar{z}$ .

To solve the Langevin equation (6) numerically, we first divide the time into small intervals  $\Delta\bar{t}$ . Then, as discussed by Riskin (1989), the value of  $\bar{z}$  at  $\bar{t} = (n + 1)\Delta\bar{t}$  can be evaluated from that at  $\bar{t} = n\Delta\bar{t}$  according to

$$\bar{z}_{n+1} = \bar{z}_n + D^{(1)}\Delta\bar{t} + \sqrt{2D^{(2)}\Delta\bar{t}}w_n.\quad (7)$$

Here  $\{w_0, w_1, \dots\}$  are independent Gaussian-distributed random variables with zero mean and with variance 1,  $\langle w_n \rangle = 0$  and  $\langle w_n w_m \rangle = \delta_{nm}$ , and  $D^{(1)}$  and  $D^{(2)}$  are respectively the first- and the second-order Kramer-Moyal expansion coefficients of Eq. 6:  $D^{(1)} = (D/k_B T)[\bar{F} - \bar{K}\bar{z}]$  and  $D^{(2)} = D$  (see Riskin (1989)). Thus, in dimensionless quantities, Eq. 7 becomes

$$z_{n+1} = z_n + [F - Kz_n]\Delta t + \sqrt{2\Delta t}w_n.\quad (8)$$

Here  $F = \bar{F}L/k_B T$  is dimensionless. From Eq. 8 one can generate a series of  $z$  values at  $t = \Delta t, 2\Delta t, \dots$  with given  $z_0$  at  $t = 0$  using the computer-generated  $\{w_0, w_1, \dots\}$ . The computer program to generate  $\{w_0, w_1, \dots\}$  can be found in the book by Press (1986).

## Monte Carlo simulation of the cycle turnover rate

In this section we show how to use the Monte Carlo method to simulate a long random walk on the mechanochemical cycle shown in Fig. 1 A with time-dependent rate constants given in Eq. 3. From this random walk the trace of the motor and that of the bead can be obtained as a function of time. In addition, the distribution of the cycle time for the motor to complete a forward cycle (an  $\alpha$  transition followed by a  $\beta$  transition) can also be obtained.

The simulation contains two steps: 1) to evaluate the "dwell" time for the motor to stay in a given state before transition to another state occurs and 2) to determine which state transition will occur at the end of the dwell time. Because state transitions of the motor are stochastic, the dwell time is a random variable. Let  $f_i(t)$  ( $i = 1, 2$  for the current model) denote the *distribution density function* of the dwell time  $t$  when the motor is in state  $i$ , and let  $R_i(\tau)$  represent the sum of all out-going *time-dependent* rate constants of the motor in state  $i$  at time  $\tau$ :

$$\begin{aligned}R_1(\tau) &= \alpha_+(z(\tau)) + \beta_-(z(\tau)), \\ R_2(\tau) &= \alpha_-(z(\tau)) + \beta_+(z(\tau))\end{aligned}\quad (9)$$

where  $z(\tau)$  is the time-dependent strain of the elastic element at time  $\tau$  as discussed in the previous section. Then,  $f_i(t)$  is related to  $R_i(\tau)$  as:

$$f_i(t) = R_i(t) \exp\left(-\int_0^t R_i(\tau) d\tau\right). \quad (10)$$

Note that when  $R$  is a constant, independent of time, the dwell time is exponentially distributed. With a given  $f_i(t)$ , the random dwell time  $T$  can be obtained from the equation

$$\int_0^T f_i(t) dt = \text{Ran} \quad (11)$$

where Ran is a random number evenly distributed between 0 and 1. Thus, using the  $z(0)$ ,  $z(\Delta\tau)$ ,  $z(2\Delta\tau)$ , ... etc. generated from Eq. 8, the dwell time  $T$  can be evaluated from Eqs. 10 and 11 using any numerical quadrature procedure. In this study we have used Simpson's rule to evaluate the integrals in Eqs. 10 and 11. After the dwell time is evaluated, a state transition is then selected using a random number and the transition rate constants evaluated at that time. By repeating these two steps, a time series (history) of state transitions on the mechanochemical cycle can be obtained.

To obtain the velocity of the motor, we have to record the positions of the bead and the neck of the motor as a function of time during the entire simulation run. At any given time the position of the center of the bead,  $x_b(t)$ , is related to that of the neck of the motor,  $x_m(t)$ , as  $x_b(t) = x_m(t) - z(t) - l_0$ , where  $l_0$  is the resting length of the spring (note: all the quantities are made dimensionless by dividing by  $L$ ). Note that it is not necessary to know  $l_0$  because it is not involved in the simulation. The value of  $l_0$  is required only when the traces of the positions of the motor and the bead are to be plotted together in the same figure (see Fig. 2). Before the motor makes a state transition  $x_m(t)$  remains constant, but  $x_b(t)$  will fluctuate as  $z(t)$ . At the moment the motor makes a state transition, both  $x_m(t)$  and  $z(t)$  change instantaneously by  $\pm a$  or  $\pm(1-a)$ , depending on the type of the transition, and this new  $z(t)$  becomes the new  $z_0$  for the evaluation of the next dwell time. To ensure that the steady state is obtained, the first 1000 completed cycles of the simulation are discarded before the positional traces of the motor and the bead are recorded for analysis. In general, the smaller the  $\Delta t$  value used in the simulation, the more accurate the simulation results are, but a longer computer time is required. For all the calculations carried out in this study,  $\Delta t = 0.001$  was used (corresponding to a time interval with dimension of  $2.13 \times 10^{-7}$  s at  $D = 3 \times 10^{-9}$  cm<sup>2</sup>/s).

Note that the procedure presented above is not the only method to simulate the time evolution of a kinetic system. Another method to obtain the time series of state transitions is to evaluate all the transition probabilities at a small time  $\Delta t$  and compare each probability with a random number (Brokaw, 1976, 1995, 2000; Pate and Cooke, 1991). It is not clear which method is more computer-efficient.

## Randomness from the chemical-kinetic formalism

In the chemical-kinetic formalism, the four load-dependent rate constants of the two-state model in Fig. 1 can be expressed as:

$$\begin{aligned} \alpha_+ &= k_+^\alpha e^{-Fa\delta_\alpha}, & \alpha_- &= k_-^\alpha e^{Fa(1-\delta_\alpha)}, \\ \beta_+ &= k_+^\beta e^{-F(1-a)\delta_\beta}, & \beta_- &= k_-^\beta e^{F(1-a)(1-\delta_\beta)}, \end{aligned}$$

**TABLE 1** The reference set of parameters used in the calculation

$D_0 = 3 \times 10^{-9}$ cm <sup>2</sup> /s	$K = 16$ ( $\bar{K} = 1.03$ pN/nm)
$L = 8$ nm	$a = 0.5$
$\delta_\alpha = 0.5$	$\delta_\beta = 0.13$
$\bar{k}_+^\alpha = 3.75$ [T] s <sup>-1</sup>	$\bar{k}_-^\alpha = 3.4 \times 10^{-2}$ s <sup>-1</sup>
$\bar{k}_+^\beta = 141.1$ s <sup>-1</sup>	$\bar{k}_-^\beta = 4.7 \times 10^{-3}$ s <sup>-1</sup>

[T] = Concentration of ATP in  $\mu\text{M}$ .

where  $F$  is the external force applied to the bead. Then, according to Fisher and Kolomeisky (1999b), the randomness of this model can be evaluated from the equation,

$$r = \frac{(\Gamma + 1)\sigma - 2(\Gamma - 1)^2\omega}{(\Gamma - 1)\sigma} \quad (12)$$

where  $\Gamma = \alpha_+\beta_+/\alpha_-\beta_-$ ,  $\sigma = \alpha_+ + \alpha_- + \beta_+ + \beta_-$ , and  $\omega = \alpha_-\beta_-/\sigma$ .

## MODEL CALCULATION RESULTS

In this section we present some of the simulation results obtained for the simple two-state kinetic cycle shown in Fig. 1 using the same set of parameters listed in Table 1, used before in paper I (Chen and Yan, 2001). The purpose is to illustrate how the randomness of the movement of the motor is affected by the diffusion coefficient of the bead ( $D$ ) and the stiffness of the spring ( $K$ ). Before doing that, we would like to briefly discuss the meaning of the  $K$  used in this study. Although it is referred to as the stiffness of the spring,  $K$  actually contains three components: the actual stiffness of the elastic spring  $K_e$ , the stiffness of the attached motor  $K_m$ , and the stiffness of the optical trap  $K_t$  that serves as the force clamp for the bead. The first two components are in series and the third one is in parallel to the first two. Thus, the resultant stiffness of the system is equal to  $K = K_e K_m / (K_e + K_m) + K_t$ . In general, to increase the trap sensitivity,  $K_t$  is usually small ( $\approx 0.037$  pN/nm, Visscher et al., 1999). Thus, if  $K_m \gg K_e \gg K_t$ , then  $K \approx K_e$ . However, if  $K_e \gg K_m \gg K_t$ , then  $K \approx K_m$ . That is,  $K$  is equal to the stiffness of the elastic element only when  $K_m \gg K_e \gg K_t$ .

## Displacements of the bead and the motor

Traces of displacements of the motor and the bead obtained at different values of  $D$  and  $K$  for the model at  $\bar{F} = 3.59$  pN and  $[T] = 2000$   $\mu\text{M}$  are shown as a function of time in Fig. 2. From a large ensemble of these traces, both the mean velocity and the randomness of the velocity of the motor can be evaluated. Several interesting results are obtained from these traces. 1) The general appearance of the bead displacement trace generated from our Monte Carlo simulations for the reference case at  $[T] = 2000$   $\mu\text{M}$ , as shown in the first picture of the upper panel, is very similar to that measured by Visscher et al. for conventional kinesins shown in their Fig. 1 (Visscher et al., 1999). 2) As one can see from the first picture of panel A, although our model contains two

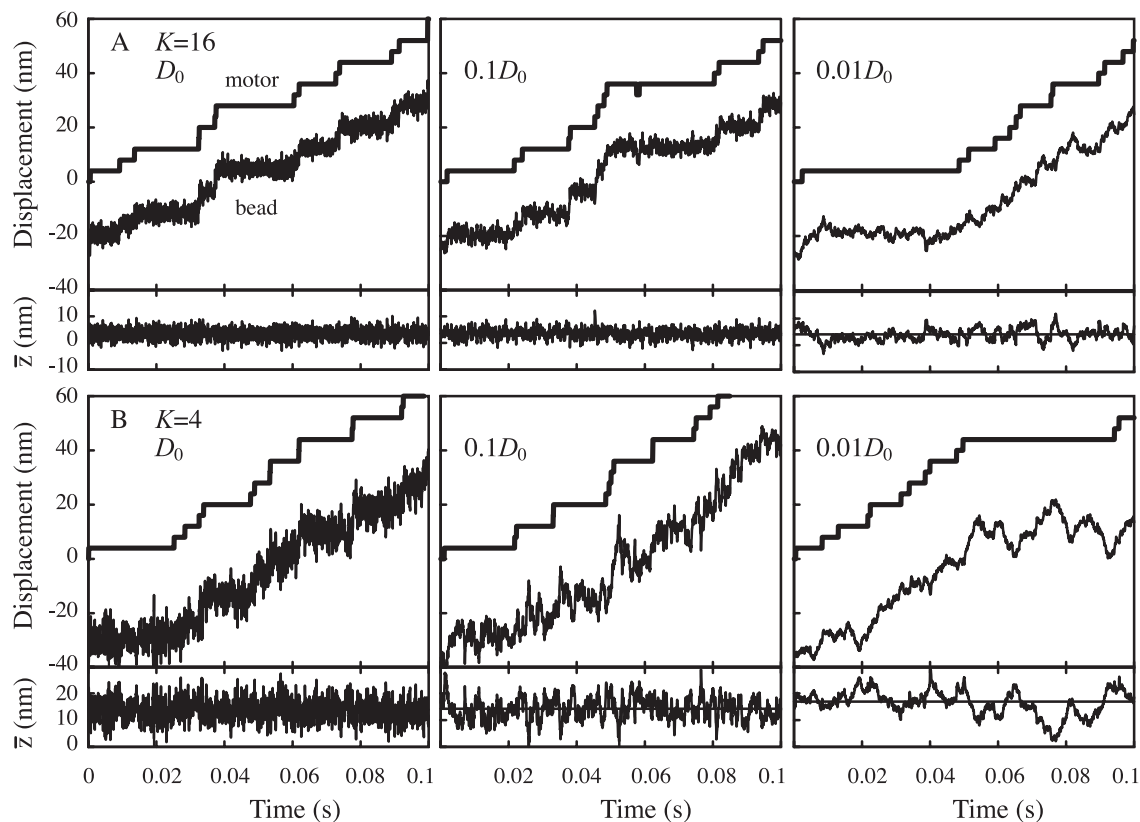


FIGURE 2 Sample records of displacements of the motor and the bead evaluated at different values of  $K$  and  $D$ . The ATP concentration and the external force applied to the bead used in the calculations are  $[T] = 2000 \mu\text{M}$  and  $\bar{F} = 3.59 \text{ pN}$ . The values of the  $D$  and  $K$  are indicated in the figure where  $D_0 = 3 \times 10^{-9} \text{ cm}^2/\text{s}$ . The time-dependent strain of the spring,  $\bar{z}(t)$ , evaluated for each case is shown at the bottom of each panel. All the data were recorded at a frequency of 20 kHz from simulations after the first 1000 cycle completions were removed and the displacements of the motor and the bead were plotted together using  $l_0 = 20 \text{ nm}$ . Note the value of  $l_0$  is not required in calculating the displacement traces (see text).

4-nm substeps for each ATPase cycle (see Fig. 1), half-step displacements are rarely seen in the trace. Most steps are 8 nm in size. This is due to the fact that  $\alpha_+$  is much larger than  $\beta_+$ , so that the motor stays in state 1 only transiently. 3) The general feature of the bead displacement trace does not change too much when the ATP concentration is reduced to  $20 \mu\text{M}$  (data not shown), except that the half-step displacement of the bead and the motor becomes obvious. 4) As the stiffness of the spring is reduced (from  $K = 16$  to  $K = 4$ ), the fluctuation of the bead displacement increases. However, the correlation between the steps of the bead and the motor is still visible (compare the first pictures in panel A and B). 5) However, the trace of the bead displacement changes drastically as the diffusion coefficient of the bead is reduced more than 10-fold: steps in the trace of the bead displacement are no longer clear-cut and are not clearly correlated with the stepwise movement of the motor.

### Strain and force fluctuations of the spring

Also shown in Fig. 2 are records of time-dependent fluctuations of the strain,  $\bar{z}(t)$ , of the spring caused by the Brown-

ian motion of the bead. The strain fluctuation in the spring causes the force exerted on the motor to fluctuate. Because our main aim in this paper is to study the effect of the force fluctuation on the cycling rate of the motor, it is important to study how the fluctuations of the strain and the force in the spring are affected by the values of  $D$  and  $K$ . Fig. 3, A–D show the distribution of the amplitudes of  $\bar{z}(t)$  evaluated from the Monte Carlo simulations at 5 kHz band width at different values of  $[T]$ ,  $K$ , and  $D$ . As one can see from the figures, the distribution of the strain amplitude becomes broader and the whole curve shifts toward the right (higher value of  $z$ ) as  $K$  or  $D$  decreases, and this effect is proportional to the concentration of ATP (or the velocity of the motor). However, one must note that the effect of  $D$  on the strain is not noticeable if  $D$  is reduced only by 10 times from the reference value ( $D_0 = 3 \times 10^{-9} \text{ cm}^2/\text{s}$ ). The strain distribution curves can be converted into the distribution of the force generated in the spring (or the force exerted on the motor) as shown in Fig. 3, E and F. Interestingly,  $K$  seems to mostly affect the shape of the distribution (variance) and  $D$  mostly affects the mean value: the distribution becomes narrower (sharper) as  $K$  decreases and the mean value of the

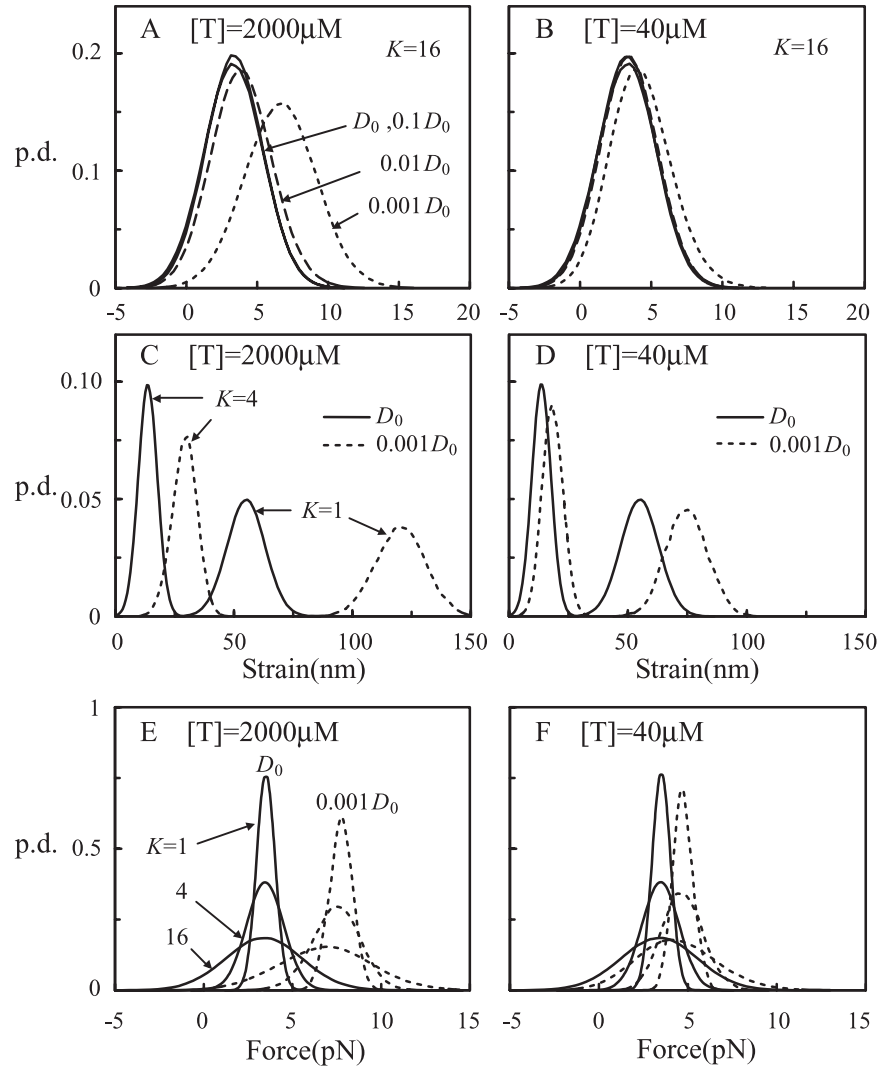


FIGURE 3 Strain and force probability density (pd) functions of the spring evaluated at different values of  $K$  and  $D$ . The pd of the strain shown in (A)–(D) was evaluated directly from the  $\bar{z}(t)$  records in Fig. 2 at a rate of 5 kHz and was converted to force in (E) and (F) by multiplying by  $K$ . The external force was fixed at  $\bar{F} = 3.59$  pN and the concentration of ATP was fixed either at 2000  $\mu\text{M}$  (left panels) or at 40  $\mu\text{M}$  (right panels). Solid curves are for  $D = D_0 (= 3 \times 10^{-9} \text{ cm}^2/\text{s})$ , the reference value and dotted curves are for  $D = 0.001 D_0$ . The values of  $K$  are indicated in the figures.

force increases as  $D$  decreases. Furthermore, the effect of  $K$  on the shape of the distribution is not greatly influenced by the ATP concentration (or the velocity of the motor), while the effect of  $D$  on the mean force is (compare Fig. 3, E and F).

To quantitatively characterize the strain fluctuation, we have evaluated  $\langle \bar{z} \rangle$  and  $\sigma_{\bar{z}}^2$  from the distribution density curves in Fig. 3. They are plotted as a function of  $D$  for the  $\bar{F} = 3.59$  pN case in Figs. 4, A and B for three  $K$  values at  $[T] = 40$  and 2000  $\mu\text{M}$ , respectively. Also shown in each figure are the corresponding equilibrium mean and variance of the strain of the spring evaluated in the absence of the movement of the motor (represented by the closed circles on the right vertical axis) [see Wang and Uhlenbeck (1945)]:

$$\langle \bar{z} \rangle_{\text{eq}} = \bar{F}/\bar{K}, \quad (13)$$

$$(\sigma_{\bar{z}}^2)_{\text{eq}} = k_B T/\bar{K}, \quad (14)$$

where  $\bar{F}$  is the external force applied to the bead. One must note that Eqs. 13 and 14 apply only when the stiffness of the

spring is linear (i.e., Hooke's law applies). If the stiffness of the spring is nonlinear, these two quantities can be evaluated by Monte Carlo simulation.

As one can see from Figs. 4, A and B, both  $\langle \bar{z} \rangle$  and  $\sigma_{\bar{z}}^2$  increase as  $K$  decreases at given  $D$  and  $[T]$ . This is not surprising, because for a Brownian particle connected to a spring the displacement of the particle in general is inversely proportional to the stiffness of the spring. An interesting finding is that the spring seems to behave quite differently depending on whether the diffusion coefficient of the bead is larger or smaller than the reference value,  $D_0 = 3 \times 10^{-9} \text{ cm}^2/\text{s}$ : at  $D \geq D_0$  both  $\langle \bar{z} \rangle$  and  $\sigma_{\bar{z}}^2$  evaluated at a given  $K$  do not depend on the values of  $D$  and  $[T]$  and are approximately equal to the "equilibrium" values evaluated from Eqs. 13 and 14, respectively; while at small  $D$  both  $\langle \bar{z} \rangle$  and  $\sigma_{\bar{z}}^2$  increase as  $D$  decreases with an increase that is proportional to the value of  $[T]$ . That is, when  $D$  is equal to or greater than  $D_0$ , the dynamic properties of the spring is completely determined by the Brownian motion of the

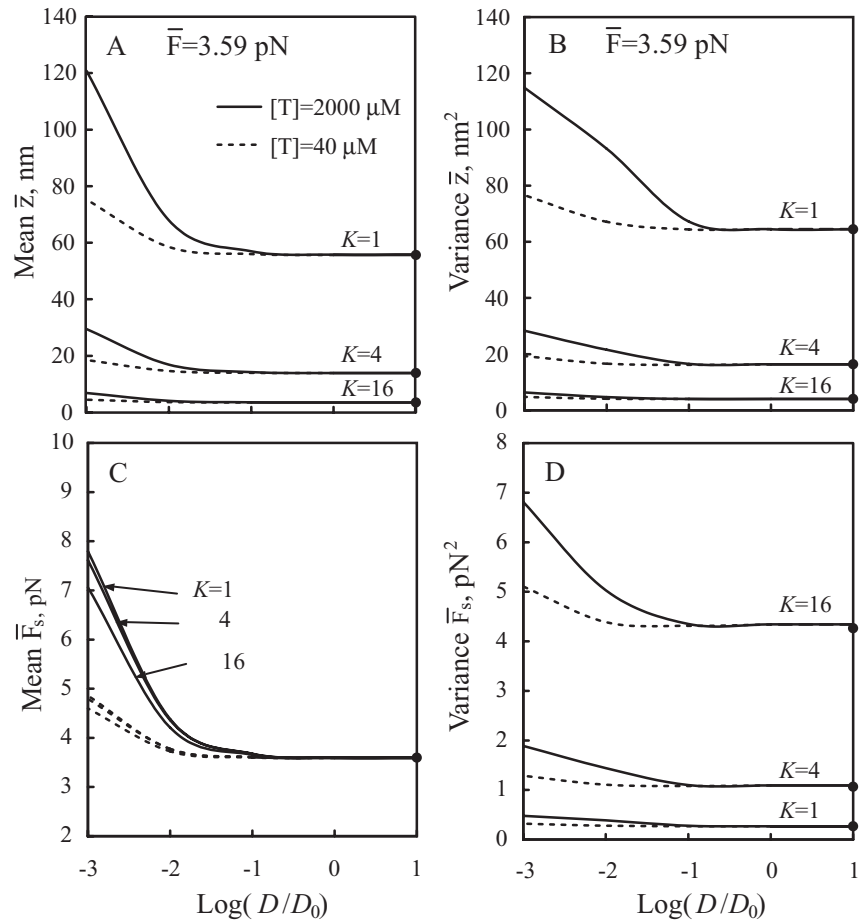


FIGURE 4 The mean and the variance of the strain  $z(t)$  (A and B) and the force in the spring (C and D) evaluated from the probability density functions in Fig. 3 at  $\bar{F} = 3.59$  pN. Solid curves are for  $[T] = 2000 \mu\text{M}$  and dotted curves are for  $[T] = 40 \mu\text{M}$ . The closed circles on the right vertical axis in each figure are evaluated for the case that the motor in the assay is not moving (from Eqs. 13 and 14).

bead, independent of the movement of the motor. In contrast, the dynamic behavior of the spring depends on both the movement of the motor and the bead when  $D$  is very small. This result is due to the fact that the relative rates of the relaxation of the spring and the turnover of the motor are very different at high and low  $D$  values. For example, at  $K = 16$  and  $D = D_0 = 3 \times 10^{-9} \text{ cm}^2/\text{s}$ , the time constant of relaxation of the spring is equal to  $KD/L^2 \approx 75,000 \text{ s}^{-1}$ , which is much larger than the cycling rate constant of the motor:  $(\bar{k}_+^\alpha \bar{k}_+^\beta - \bar{k}_-^\alpha \bar{k}_-^\beta) / (\bar{k}_+^\alpha + \bar{k}_+^\beta + \bar{k}_-^\alpha + \bar{k}_-^\beta) \approx 140 \text{ s}^{-1}$  at  $[T] = 3 \text{ mM}$ . This is true even when  $K$  is reduced from 16 to 1. Thus, at  $D \geq D_0$  the bead can relax to its “equilibrium” position quickly after each translocation event of the motor. As a result, the translocation of the motor contributes very little to the fluctuation of the strain of the spring, so that both  $\langle \bar{z} \rangle$  and  $\sigma_{\bar{z}}^2$  are approximately equal to those evaluated from Eqs. 13 and 14, respectively. However, when  $D$  is greatly reduced so that the two rate constants become comparable, then the fluctuation of the strain of the spring is determined not only by the Brownian motion of the bead, but also by the movement of the motor. The mean strain of the spring is larger than that from Eq. 13 because the bead cannot relax to its equilibrium position quickly after each translocation event of the motor. The

variance is larger than that from Eq. 14 because the strain fluctuation now contains contributions from both the motor and the bead.

The mean and the variance of the force fluctuations,  $\langle \bar{F}_s \rangle$  and  $\sigma_{\bar{F}_s}^2$ , obtained directly from  $\langle \bar{z} \rangle$  and  $\sigma_{\bar{z}}^2$  are shown in Fig. 4, C and D. Similar to the strain, both the mean and the variance of the force of the spring evaluated at a given  $K$  are also independent of  $D$  at high  $D$  and become inversely proportional to  $D$  when  $D$  is drastically reduced. Interestingly, the strain and the force of the spring evaluated at a given  $D$  have very different  $K$ -dependencies. In contrast to the strain, the mean force of the spring is not very sensitive to the value of  $K$ : independent of  $K$  at  $D \geq D_0$  and only slightly dependent on  $K$  at very low  $D$  values (compare Fig. 4, A and C). However, similar to the strain, the variance of the force is very sensitive to the value of  $K$  at any given  $D$ . However, as can be seen from Fig. 4, B and D, the  $K$ -dependency is very different for the two variances: as  $K$  increases,  $\sigma_{\bar{z}}^2$  decreases while  $\sigma_{\bar{F}_s}^2$  increases.

### The randomness of the motor movement

Let  $x(t)$  denote the distance traveled by the bead in time  $t$  obtained from the time series of displacements of the bead

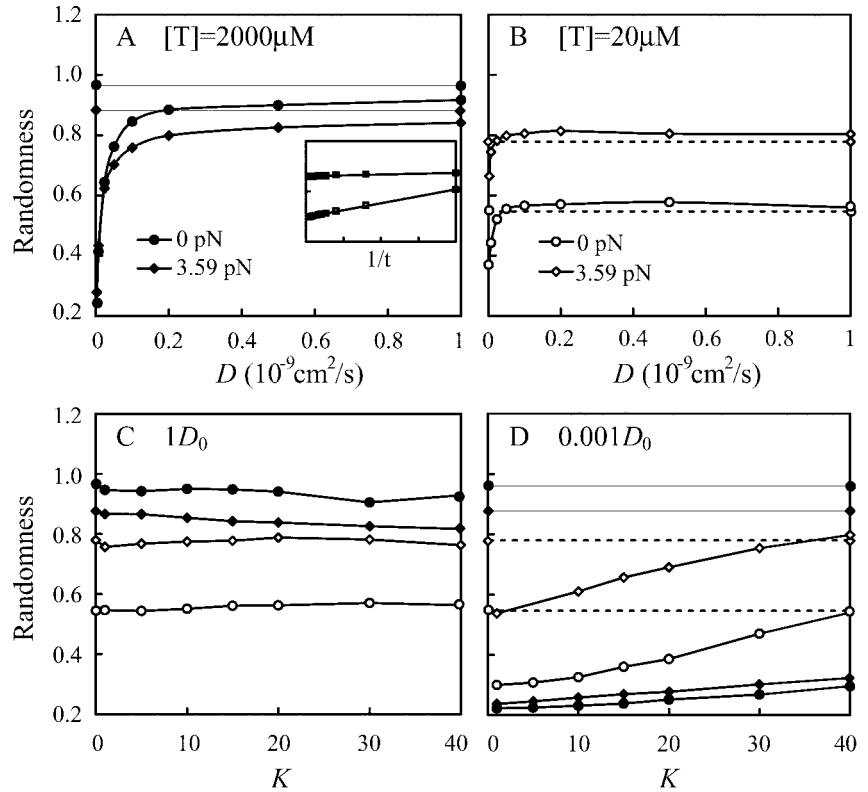


FIGURE 5 The randomness as a function of  $D$  (in *A* and *B*) and as a function of  $K$  (in *C* and *D*) at  $\bar{F} = 3.59$  pN (diamonds) and  $\bar{F} = 0$  pN (circles) and  $[T] = 2000 \mu\text{M}$  (filled symbols) and  $[T] = 20 \mu\text{M}$  (open symbols). The values of the randomness evaluated using the chemical-kinetic (CK) formalism are independent of  $D$  and  $K$  and are shown in thin (for  $[T] = 2000 \mu\text{M}$ ) and dashed ( $[T] = 20 \mu\text{M}$ ) lines in (*A*), (*B*), and (*D*). Inset: the extrapolation method used to obtain the randomness at infinite times.

as shown in Fig. 2. Then, the randomness  $r$  of the velocity of the bead is defined as (Visscher et al., 1999)

$$r = \lim_{t \rightarrow \infty} \frac{\langle x^2(t) \rangle - \langle x(t) \rangle^2}{L \langle x(t) \rangle}, \quad (15)$$

where the angle brackets denote an ensemble average. One must note that at long time the distance traveled by the bead and that by the motor are practically identical. Therefore, for a processive motor, the randomness is also defined as

$$r = \lim_{t \rightarrow \infty} \frac{\langle n^2(t) \rangle - \langle n(t) \rangle^2}{\langle n(t) \rangle}. \quad (16)$$

where  $n(t)$  is the number of cycles completed by the motor in  $t$ .

Because we cannot obtain ensemble averages of  $x(t)$  (or  $n(t)$ ) in the limit of  $t \rightarrow \infty$ , the randomness was obtained by extrapolation. That is, the value of  $r$  at finite times,  $r(t)$ , was first evaluated from displacement records such as those shown in Fig. 2 for a number of  $t$  values and plotted as a function of  $1/t$ . The randomness is then equal to the intercept at  $1/t = 0$  (see the inset in Fig. 5). In general, each ensemble contains 20,000 simulation runs. The randomness evaluated is plotted as a function of  $D$  in Fig. 5, *A* and *B* and as a function of  $K$  in Fig. 5, *C* and *D*. Several interesting results can be seen from these figures. First, similar to the mean velocity as found in paper I, the randomness of the velocity evaluated at fixed  $K$ ,  $F$ , and

$[T]$  also decreases slightly as the diffusion coefficient  $D$  is slightly reduced from the reference value of  $3 \times 10^{-9} \text{cm}^2/\text{s}$ . A pronounced decrease occurs only after  $D$  is reduced by more than 10-fold (see Fig. 5, *A* and *B*). Curves of randomness as a function of  $D$  have also been obtained for  $K = 4$  (data not shown). The shapes of the curves are very similar, except that the randomness values are relatively smaller. Second, randomness evaluated at fixed  $D$ ,  $F$ , and  $[T]$  seems less affected by the stiffness of the spring if the diffusion coefficient is equal to or larger than the reference  $D_0$ , as can be seen from Fig. 5 *C*. In contrast, the randomness decreases as  $K$  decreases if  $D$  is reduced 1000-fold from the reference value (see Fig. 5*D*). Third, the randomness evaluated based on the chemical-kinetic (CK) formalism of Fisher and Kolomeisky (1999b) is different from that evaluated using the Monte Carlo (MC) method. As shown in Fig. 5, *A* and *B*, the randomness evaluated at high  $D$  (equal to or larger than  $D_0$ ) using the CK formalism may be slightly larger or smaller than the actual MC value, depending on the value of  $[T]$ . And, when the value of  $D$  is  $< 0.1 D_0$ , the CK formalism always largely overestimates the actual randomness (see Fig. 5 *D*). That is, the CK formalism is expected to generate erroneous randomness when the diffusion coefficient of the bead is very small. This conclusion does not depend on the value of  $K$ , as can be seen from Fig. 5 *D*.



## DISCUSSION AND CONCLUSIONS

The ultimate aim of this series of studies is to elucidate the load-dependent mechanochemical cycle of kinesin (or other processive) motors using data obtained from biochemical studies and in vitro motility assays. Data from the VSB motility assay (Visscher et al., 1999), in which the movement of a bead attached elastically to a single moving motor can be monitored under a force clamp, are especially useful for this purpose because the load carried by the motor can be manipulated externally. However, because the bead in the VSB assay is free to undergo Brownian motions, the force exerted on the motor by the bead is not constant, but fluctuates randomly. Thus, in modeling with the VSB data one needs a formalism that takes into account explicitly the hydrodynamic behavior of the bead. One of the purposes of this paper and paper I (Chen and Yan, 2001) is to derive such a formalism. That is, we are interested in procedures that can be used to calculate the velocity of the motor and the bead when both the hydrodynamic parameters of the system and the kinetic parameters of the “mechanochemical” cycle of the motor are given. In paper I, we solved the Fokker-Planck equations for the bead and derived a semi-analytic formalism that can be used to calculate the *mean velocity* of the motor. In this paper, we present a Monte Carlo procedure that can evaluate not only the *mean* but also the *variance (dispersion or randomness)* of the velocity of the motor.

### Load fluctuation generates different effects on the mean and the randomness of the motor movement

In addition to formulating the procedure, another purpose of this paper is to study how the randomness of the velocity of the motor is affected by the Brownian motion of the cargo (or the bead in the VSB assay) it carries. In particular, we want to compare how the mean velocity and the randomness of the movement of the motor are affected by the load fluctuations.

As shown in Fig. 5, *A*, and *B*, the *D*-dependence of the randomness is very similar to that of the mean velocity: the randomness remains relatively unchanged as *D* is varied near the reference value of  $D_0 = 3 \times 10^{-9} \text{ cm}^2/\text{s}$  and drops sharply after *D* is reduced more than 10-fold. A similar result has also been obtained for the case with a reduced *K* ( $K = 4$ , data not shown). In contrast, the *K*-dependence of the randomness is quite different from that of the mean velocity. As shown in Fig. 5, *C* and *D*, the randomness remains relatively constant as a function of *K* at  $D_0$  and *decreases* almost linearly as *K* decreases at  $D = 0.001 D_0$ . This result implies that the randomness is very sensitive to the mean value of the load exerted on the motor, but not sensitive to the fluctuation of the load. This conclusion can be easily realized if one examines the *K*-dependencies of the

mean and the variance of the force fluctuations at high and low *D* values shown in Fig. 4, *C* and *D*: the variance depends on *K* at any *D* value, while the mean depends on *K* only at very low *D* values. However, the mean velocity of the motor is sensitive to both the mean and the variance of the load applied to the motor, because the mean velocity of the motor was found to be inversely proportional to the value of *K* at both  $D = D_0$  (see Fig. 2 of paper I) and  $D = 0.001 D_0$  (data not shown). Thus, it is concluded that the fluctuation of the load produces different effects on the mean velocity and the randomness of the movement of the motor. This result highlights the importance of studying both the mean and the randomness of the velocity as a function of the hydrodynamic parameters of the system, such as the size of the bead, the viscosity of the medium, and the stiffness of the elastic element, etc., when modeling the kinetic mechanism of processive motors.

However, we do not know exactly why the randomness decreases as a function of *K* at low *D* as shown in Fig. 5*D*. In general, the randomness of the velocity of a motor is approximately inversely proportional to the *number* of “rate-limiting” steps in the mechanochemical cycle of the motor (Svoboda and Block, 1994; Schnitzer and Block, 1995), if the hydrodynamic interaction of the bead is neglected. This is the reason that the randomness calculated using the “chemical-kinetic” formalism for this two-state model is always larger than 0.5 (see the thin and dotted lines in Fig. 5, *A–D*). Why the randomness can be reduced even below 0.5 at small *D* for this two-state model as shown in Fig. 5*D* is an interesting problem remaining to be studied.

### Does a motor move faster or slower when neglecting the Brownian motion of the cargo?

Because the cargo (or bead) carried by a biological motor in vivo (or in vitro motility assays) is constantly undergoing Brownian motion (this is the difference between a macroscopic and a microscopic motor system), it is interesting to know whether the *presence* of the Brownian motion increases or decreases the velocity of the motor. As shown in paper I, the velocity of the motor in the VSB assay was found to increase when the stiffness of the spring *K* is reduced or when the diffusion coefficient of the bead *D* is increased. Because reducing *K* or increasing *D* in general increases the amplitude of the Brownian motion of the bead, one might conclude that the motor moves faster in the presence of the Brownian motion of the bead. However, it is the fluctuation of the “force” exerted on the motor, not that of the displacement of the bead, that is *directly* involved in the turnover of the motor. Thus, to answer the above question, one must look at the effect of *K* and *D* on the fluctuation of the *force* (or *stress*) of the elastic spring. Because *K* affects mostly the *fluctuation* of the force as discussed in the previous section (or see Fig. 4, *C* and *D*), it is sufficient to use the *K*-dependence to examine how the motor turnover

rate is affected by the force fluctuation of the spring. As shown in paper I, the movement of the motor slows down when the value of  $K$  increases. Thus, from Fig. 4  $D$  we conclude that the motor moves slower as the force fluctuation becomes larger. In other words, the *presence* of fluctuation of the force in the elastic spring caused by the *presence* of the Brownian motion of the bead should *decrease*, rather than *increase*, the turnover rate of the motor. However, because the force fluctuation becomes smaller when  $K$  is reduced, the reduction in motor velocity by the presence of the Brownian motion of the bead becomes smaller when the Brownian motion is increased. That is, when attached with a cargo, the velocity of a motor slows down if the cargo is allowed to undergo Brownian motion, but the degree of the slow-down is reduced when the Brownian motion becomes larger. This is the reason why the velocity of the motor evaluated using the “chemical-kinetic” formalism, in which the Brownian motion of the bead is neglected, is always an overestimate, as shown in Fig. 5 of paper I.

### The procedure can be useful in estimating the values of $K$ and $D$

The fact that both  $K$  and  $D$  have an effect on both the mean and the randomness of the velocity of motor implies that, before single-motor motility data can be used to deduce the kinetic mechanism of the motor, it is important to determine the values of these two parameters present in the motility assay. In general, these two parameters can be determined by analyzing the displacement fluctuations of the bead (which is identical to the strain fluctuations of the spring). If the spring is linear (obeys Hooke’s law) and the motor is not moving, the values of  $K$  and  $D$  can be obtained from the measured strain fluctuations using Eq. 14 and the following equation:

$$\tau = \frac{L^2}{KD}$$

where  $\tau$  is the (measured) decay time constant of the *time-correlation* function of the strain fluctuation (Howard, 2001). However, if the strain fluctuations are measured in the presence of movement of the motor or if the spring is nonlinear, the values of these two parameters can be estimated by numerical model simulations. In this case, the Monte Carlo method presented in this paper becomes very useful.

### REFERENCES

- Brokaw, C. J. 1976. Computer simulation of movement-generating cross-bridges. *Biophys. J.* 16:1013–1027.
- Brokaw, C. J. 1995. Weakly-coupled models for motor enzyme function. *J. Muscle Res. Cell Motil* 16:197–211.
- Brokaw, C. J. 2000. Stochastic simulation of processive and oscillatory sliding using a two-headed model for axonemal dynein. *Cell Motil. Cytoskel.* 47:108–119.
- Chen, Y., and B. Yan. 2001. Theoretical formalism for bead movement powered by single two-headed motors in a motility assay. *Biophys. Chem.* 91:79–91.
- Coppin, C. M., D. W. Pierce, L. Hsu, and R. D. Vale. 1997. The load dependence of kinesin’s mechanical cycle. *Proc. Natl. Acad. Sci. USA.* 94:8539–8544.
- Cross, R. A. 1995. On the hand-over-hand footsteps of kinesin heads. *J. Muscle Res. Cell Motil.* 16:91–94.
- Fisher, M. E., and A. B. Kolomeisky. 1999a. The force exerted by a molecular motor. *Proc. Natl. Acad. Sci. USA.* 96:6597–6602.
- Fisher, M. E., and A. B. Kolomeisky. 1999b. Molecular motors and the forces they exert. *Physica A.* 274:241–266.
- Fisher, M. E., and A. B. Kolomeisky. 2001. Simple mechanochemistry describes the dynamics of kinesin molecules. *Proc. Natl. Acad. Sci. USA.* 98:7748–7753.
- Gelles, J., E. Berliner, E. C. Young, H. K. Mahtani, B. Perez-Ramirez, and K. Anderson. 1995. Structural and functional features of one- and two-headed biotininated kinesin derivatives. *Biophys. J.* 68:276S–281S.
- Hancock, W. O., and J. Howard. 1999. Kinesin’s processivity results from mechanical and chemical coordination between the ATP hydrolysis cycles of the two motor domains. *Proc. Natl. Acad. Sci. USA.* 96:13147–13152.
- Howard, J. 2001. *Mechanics of Motor Proteins and the Cytoskeleton*, Chapt. 2 and Appendix 2.1 Sinauer Associates, Inc., Sunderland, MA.
- Kojima, H., E. Muto, H. Higuchi, and T. Yanagida. 1997. Mechanics of single kinesin molecules measured by optical trapping nanometry. *Biophys. J.* 73:2012–2022.
- Kolomeisky, A. B., and B. Widom. 1998. A simplified “Ratchet” model of molecular motors. *J. Stat. Phys.* 93:633–645.
- Mehta, A. 2001. Myosin learns to walk. *J. Cell Sci.* 114:1981–1998.
- Pate, E., and R. Cooke. 1991. Simulation of stochastic processes in motile crossbridge systems. *J. Mus. Res. Cell Mot.* 12:376–393.
- Peskin, C. S., and G. Oster. 1995. Coordinated hydrolysis explains the mechanical behavior of kinesin. *Biophys. J.* 68:202S–210S.
- Press, W. H. 1986. *Numerical Recipes: The Art of Scientific Computing*. Cambridge University Press, New York.
- Qian, H. 1997. A simple theory of motor protein kinetics and energetics. *Biophys. Chem.* 67:263–267.
- Qian, H. 2000. A simple theory of motor protein kinetics and energetics. II. *Biophys. Chem.* 83:35–43.
- Rice, S., A. W. Lin, D. Safer, C. L. Hart, N. Naber, B. O. Carragher, S. M. Cain, E. Pechatnikova, E. M. Wilson-Kubalek, M. Whittaker, E. Pate, R. Cooke, E. W. Taylor, A. Milligan, and R. D. Vale. 1999. A structural change in the kinesin motor protein that drives motility. *Nature.* 402:778–784.
- Rief, M., R. S. Rock, A. D. Mehta, M. S. Mooseker, R. E. Cheney, and J. A. Spudich. 2000. Myosin-V stepping kinetics: a molecular model for processivity. *Proc. Natl. Acad. Sci. USA.* 97:9482–9486.
- Risken, H. 1989. *The Fokker-Planck Equation*, 2nd Ed., chapt. 3. Springer-Verlag, New York.
- Romberg, L., D. W. Pierce, and R. D. Vale. 1998. Role of the kinesin neck region in processive microtubule-based motility. *J. Cell Biol.* 140:1407–1416.
- Schief, W. R., and J. Howard. 2001. Conformational changes during kinesin motility. *Curr. Opin. Cell Biol.* 13:19–28.
- Schnitzer, M. J., and S. M. Block. 1995. Statistical kinetics of processive enzymes. *Cold Spring Harbor Symp. Quant. Biol.* 60:793–802.
- Schnitzer, M. J., K. Visscher, and S. M. Block. 2000. Force production by single kinesin motors. *Nat. Cell Biol.* 2:718–723.
- Svoboda, K., and S. M. Block. 1994. Force and velocity measured for single kinesin molecules. *Cell.* 77:773–784.
- Visscher, K., M. J. Schnitzer, and S. M. Block. 1999. Single kinesin molecules studied with a molecular force clamp. *Nature.* 400:184–189.
- Wang, M. C., and G. E. Uhlenbeck. 1945. On the theory of the Brownian motion. II. *Rev. Mod. Phys.* 17:323–342.